Langevin approach to synchronization of hyperchaotic time-delay dynamics

2008 J. Phys. A: Math. Theor. 41 445001

(http://iopscience.iop.org/1751-8121/41/44/445001)

IOP PUBLISHING JOURNAL OF PHYSICS A: MATHEMATICAL AND THEORETICAL

J. Phys. A: Math. Theor. **41** (2008) 445001 (19pp) doi:10.1088/1751-8113/41/44/445001

Langevin approach to synchronization of hyperchaotic time-delay dynamics

Adrián A Budini

Consejo Nacional de Investigaciones Científicas y Técnicas, Centro Atómico Bariloche, Av. E Bustillo Km 9.5, (8400) Bariloche, Argentina
and
Consortium of the Americas for Interdisciplinary Science and Department of Physics and Astronomy, University of New Mexico, Albuquerque, NM 87131, USA

Received 10 April 2008, in final form 11 August 2008
Published 7 October 2008
Online at stacks.iop.org/JPhysA/41/445001

Abstract

In this paper, we characterize the synchronization phenomenon of hyperchaotic scalar nonlinear delay dynamics in a fully-developed chaos regime. Our results rely on the observation that, in that regime, the stationary statistical properties of a class of hyperchaotic attractors can be reproduced with a linear Langevin equation, defined by replacing the nonlinear delay force by a delta-correlated noise. Therefore, the synchronization phenomenon can be analytically characterized by a set of coupled Langevin equations. We apply this formalism to study anticipated synchronization dynamics subject to external noise fluctuations as well as for characterizing the effects of parameter mismatch in a hyperchaotic communication scheme. The same procedure is applied to second-order differential delay equations associated with synchronization in electro-optical devices. In all cases, the departure with respect to perfect synchronization is measured through a similarity function. Numerical simulations in discrete maps associated with the hyperchaotic dynamics support the formalism.

PACS numbers: 05.45.Xt, 05.45.Jn, 05.40.Ca, 05.45.Vx

1. Introduction

In the last decades, *synchronization* of chaotic dynamics became a subject that has attracted a lot of attention [1–7]. In fact, from a theoretical point of view, this phenomenon seems to contradict the inheriting sensibility to initial conditions of chaotic dynamics. On the other hand, the interest in this kind of phenomenon comes from the possibility of using the unpredictable chaotic trajectories as a carrier signal in communication channels. In this context, high-dimensional systems with multiple positive Lyapunov exponents, i.e., *hyperchaotic dynamics* [8], have been proposed as a resource for improving the security in the communication schemes.

Synchronization of hyperchaotic systems has therefore also become an area of active research [9–13].

Chaotic dynamics described by differential delay equations arise in the description of many different kinds of situations, such as physiology [14, 15], biology [16], economy [17], laser physics [18–22], etc. As is well known, a high-dimensional chaotic attractor characterizes these infinite-dimensional systems. It has been shown that the Lyapunov dimension of the attractor is proportional to the characteristic delay time of the dynamics [22–25]. Therefore, '*synchronization of hyperchaotic nonlinear delay dynamics*' has also been extensively explored from both a theoretical point of view as well as a resource for communication schemes [26–29]. A new aspect introduced in this case is the possibility of synchronizing two chaotic dynamics with a time shift, giving rise to the phenomenon of anticipated [30–40] (or retarded) synchronization, i.e., one of the chaotic systems (slave or receiver system) follows the chaotic trajectory of the other one (master or transmitter system) with an advanced (or retarded) time shift.

In any real experimental setup where chaotic synchronization is observed one is naturally confronted with two undesirable effects that avoid reaching a perfectly synchronized regime. The characteristic parameters of both systems are not exactly the same, small *parameter mismatch* may induce clearly observable effects [41–43]. Also, departure with respect to the perfectly synchronized manifold may also be due to intrinsic *noise fluctuations* present in both systems [44, 45]. Both effects have been analyzed in the literature. Nevertheless, due to the chaotic character of the dynamics, in general it is hard to obtain an analytical estimation of these effects, which in fact may depend on the specific nature of the chaotic systems as well as on the coupling scheme used to achieve synchronization.

The aim of this paper is to provide a simple analytical description of the phenomenon of synchronization of hyperchaotic delay dynamics, considering realistic situations such as the presence of parameter mismatch as well as the presence of intrinsic noise fluctuations in both synchronized systems. We demonstrate that this goal can be achieved when the synchronized dynamics are in a *fully-developed chaos regime* [46]. In this situation, the corresponding chaotic attractor does not have any stable periodic orbit and its basin of attraction fills out almost the whole available domain. These properties suggest that the nonlinear delay contribution terms of the chaotic dynamics may be statistically equivalent to an ergodic noise source. As demonstrated in [47, 48], this property, in a long-time limit and depending on the characteristic parameter values, is in fact valid for a broad class of scalar delay dynamics. Therefore, our *main idea* consists in replacing the full set of coupled delay chaotic evolutions that lead to synchronization by a set of *correlated Langevin evolutions* obtained from the original chaotic ones after replacing the nonlinear delay contributions by a noise term. Since the final Langevin equations are linear, their statistical properties can be obtained in an exact analytical way, providing a simple framework for characterizing the synchronization phenomenon. Departure with respect to perfect synchronization is characterized in terms of a *similarity function* [49], which measures the degree of correlation between the quasi-synchronized dynamics.

The paper is organized as follows. In section 2, we review the conditions under which hyperchaotic delay dynamics can be represented by a Langevin dynamics. In section 3, we analyze the phenomenon of anticipated synchronization when perturbed by external additive noises. In section 4, we analyze the effect of parameters mismatch in a hyperchaotic communication scheme [26]. In section 5, we study a set of second-order differential delay equations associated with an electro-optical laser device [43] under the effect of parameter mismatch and under the action of external additive noises. In all cases, we

present numerical simulations that sustain our theoretical results. In section 6, we give the conclusions.

2. Langevin approach to hyperchaotic delay dynamics in the fully-developed chaos regime

We will consider scalar nonlinear delay evolutions with the structure

$$\dot{u}(t) = -\gamma u(t) + \beta f[u(t-T)] + \mathrm{I}(t). \tag{1}$$

Here, γ defines a dissipative timescale and T is the characteristic time delay. The parameter β controls the weights of the nonlinear function $f(x)$, which is assumed to be *oscillatory* or at least exhibiting many different extrema[1]. The term $\mathrm{I}(t)$ represents an extra inhomogeneous contribution that may corresponds to a stationary Gaussian white noise (section 3), a deterministic signal (section 4) or even it may be a linear functional of the process $u(t)$ (section 5).

The parameter βT may be considered as a complexity control parameter. In fact, when $\beta T \gg 1$, the dynamic reaches a fully-developed chaos regime, where the stationary statistical properties of the corresponding attractor can be reproduced with a linear Langevin equation [47, 48]. This property can be understood by integrating equation (1), in *the long-time limit* ($\gamma t \gg 1$), as

$$\tilde{u}(t) \approx \int_0^t \mathrm{d}t'\, \mathrm{e}^{-\gamma(t-t')} f[\beta\tilde{u}(t'-T) + \tilde{\mathrm{I}}(t'-T)], \tag{2}$$

where $\tilde{u}(t) = [u(t) - \tilde{\mathrm{I}}(t)]/\beta$, and $\tilde{\mathrm{I}}(t)$ is defined by $\tilde{\mathrm{I}}(t) \equiv \int_0^t \mathrm{d}t'\, \mathrm{e}^{-\gamma(t-t')} I(t')$. Then, by writing the integral operation over $f(x)$ as a discrete sum, $\int_0^t \mathrm{d}t' g(t') \to \sum_j \mathrm{d}t' g(j\,\mathrm{d}t')$, one realizes that $\tilde{u}(t)$ may be considered as the result of the addition of many '*statistically independent*' contributions. This last property follows from the fact that $f[\beta x]$ oscillates so fast that it behaves as a driving random force. The characteristic correlation time (in units of time $1/\gamma$) of the nonlinear force $f[\beta x]$ is of order γ/β [47, 48]. When the correlation time is the small timescale of the problem, i.e., much shorter than the characteristic delay time, $\gamma/\beta \ll \gamma T$, and consistently much shorter than the characteristic dissipative time, $\gamma/\beta \ll 1$, the statistical independence of the different contributions follows. Note that this last property is independent of the structure of the inhomogeneous term $\tilde{\mathrm{I}}(t)$, which only introduce a shift in the argument of $f[\beta x]$.

From the previous analysis, in the parameters region $\beta T \gg 1$ and $\gamma/\beta \ll 1$, the central limit theorem [50] tells us that $\tilde{u}(t)$ is a Gaussian process. Due to this characteristic, this regime is also named *Gaussian chaos*. Only when $\tilde{\mathrm{I}}(t-T)$ is a nonlinear function (functional) of $u(t)$ [48], the long-time statistic may depart from a Gaussian one.

The lack of correlation between the different contributions of the 'chaotic force' $f[\beta\tilde{u}(t-T) + \tilde{\mathrm{I}}(t-T)]$, allows us to introduce the following ansatz. In the fully-developed chaos regime, '*the long-time statistical properties*' of $u(t)$ can be equivalently obtained from equation (2) after replacing the chaotic force by a noise contribution ($\beta f[\tilde{u}(t-T) + \tilde{\mathrm{I}}(t-T)] \to \eta(t-T)$), delivering the Langevin equation

$$\dot{u}(t) = -\gamma u(t) + \eta(t-T) + \mathrm{I}(t). \tag{3}$$

[1] There exist cases where this condition is not satisfied, as for example for the Mackey-Glass dynamic [14, 48], which arise in the context of white-blood-cell production.

The noise $\eta(t)$ must have the same statistical properties as the delayed chaotic force. Since we are restricting our analysis to the Gaussian chaos regime, it is sufficient to map the first two statistical moments[2]

$$\overline{\eta(t)} = \lim_{t\to\infty} \beta \overline{f[u(t)]}, \tag{4}$$

$$\overline{\eta(t+\tau)\eta(t)} = \lim_{t\to\infty} \beta^2 \overline{f[u(t+\tau)]f[u(t)]}. \tag{5}$$

The limit operation ($\lim_{t\to\infty}$) is introduced because the statistical mapping is only valid in the long-time regime. The overbar symbol denotes an average over realizations obtained from equation (1) with different initial conditions. Equivalently, since the chaotic attractor is ergodic (by definition of the fully-developed chaos regime) when the inhomogeneous term is statistically stationary [50], this average can also be considered as a time average. For example, $\lim_{t\to\infty} \overline{f[u(t)]} = \lim_{t\to\infty}(1/t)\int_0^t \mathrm{d}t' f[u(t')]$.

In agreement with the lack of correlation between the different contributions of the chaotic force, $\eta(t)$ can be approximated by a delta-correlated noise,

$$\overline{\eta(t)\eta(t')} - \overline{\eta(t)}\ \overline{\eta(t')} = \mathcal{A}\delta(t-t'). \tag{6}$$

This white noise approximation applies for time intervals $(t-t')$ larger than the characteristic time correlation (γ/β) (in units of time $1/\gamma$) of the chaotic force [47, 48], i.e., $\gamma(t-t') > (\gamma/\beta)$.

The coefficient $\mathcal{A}$ measures the amplitude of $f[u(t)]$. Clearly, $\mathcal{A}$ must be proportional to β^2. Nevertheless, its exact value is not universal and depends on the specific function $f(x)$ [47] as well as on the parameters that define the inhomogeneous term (see the following section).

When $\mathrm{I}(t)$ is defined by an external driving force, we will assume that

$$\overline{[\eta(t) - \overline{\eta(t)}]\mathrm{I}(t')} = 0, \tag{7}$$

i.e., the noise fluctuations representing the chaotic force and the inhomogeneous term are statistically uncorrelated. The plausibility of this assumption follows from the fact that the white nature of $\eta(t)$ only relies on the rapid oscillating nature of $f[\beta x]$ while it is not affected by the shift introduced by the functional $\tilde{\mathrm{I}}(t)$. Under this condition, the inhomogeneous contribution only affects the mean value of the Gaussian profile associated with $u(t)$.

Finally, we will assume that $\overline{\eta(t)} = 0$. The validity of this condition only depends on the specific properties of the nonlinear chaotic force. In fact, the rapid oscillating nature of $f[\beta x]$ allows us to discarding the asymmetry introduced by $\tilde{\mathrm{I}}(t)$ (equation (2)). As will become clear in the following section, the generalization to the case $\lim_{t\to\infty} \beta\overline{f[u(t)]} \neq 0$ can also be worked straightforwardly.

With the noise correlation equation (6), the stochastic evolution equation (3) becomes a (driven) Orstein–Ulenbeck process [50]. The statistical equivalence in the stationary and fully-developed chaos regimes of the deterministic evolution equation (1) and the Langevin equation (3), (without the inhomogeneous term) was proved in [47, 48]. Clearly, this stochastic representation does not provide any new information about the chaotic dynamics. Nevertheless, in the following sections we will use this equivalence for formulating a simple framework that allows us to get an analytical characterization of the chaotic synchronization phenomenon for different realistic circumstances.

[2] Strictly, the mapping defined by equations (4) and (5) is sufficient for *Markovian* Gaussian process. The Markovian property is guaranteed by the validity of the white noise approximation (equation (6)). On the other hand, we note that independently of the probability distribution associated with $\eta(t)$, by appealing to the central limit theorem [50], the correlation equation (6) guarantees that, in the long-time regime, equation (3) always converges to a Gaussian process.

3. Anticipated synchronization subject to external additive noises

In this section we will apply the previous Langevin representation of a hyperchaotic attractor to analyze the phenomenon of anticipated synchronization [30–32] in the presence of external noise sources. We consider a complete replacement scheme [39], defined by the *coupled chaotic evolutions*

$$\dot{x}(t) = -\gamma x(t) + \beta f[x(t-T)] + \xi_x(t), \tag{8a}$$

$$\dot{y}(t) = -\gamma y(t) + \beta f[x(t)] + \xi_y(t). \tag{8b}$$

In this context, the variables $x(t)$ and $y(t)$ are referred as master and slave variables, respectively. As before, γ is a constant dissipative rate and β measures the weight of the delay-nonlinear contribution $f(x)$.

We have considered external noise sources, defined by the master and slave noises $\xi_x(t)$ and $\xi_y(t)$ respectively. We assume that their mean values are null $\langle \xi_z(t) \rangle = 0$, where $z = x, y$ and $\langle \cdots \rangle$ denotes average over noise realizations. Furthermore, we assume that both noises are Gaussian, with correlations

$$\langle \xi_z(t) \xi_{z'}(t') \rangle = \mathcal{A}_{zz'} \delta(t - t'). \tag{9}$$

The 'diffusion' coefficients satisfy the positivity constraint $\mathcal{A}_{xx}\mathcal{A}_{yy} - \mathcal{A}_{xy}\mathcal{A}_{yx} \geqslant 0$, $(\mathcal{A}_{xy} = \mathcal{A}_{yx})$ [50]. These definitions allow us to cover the case where both the master and slave variables are affected by intrinsic uncorrelated fluctuations, $\mathcal{A}_{xy} = 0$, as well as the case of correlated fluctuations $\mathcal{A}_{xy} > 0$. This last situation may be easily produced in any experimental setup. In particular, for $\mathcal{A}_{xx} = \mathcal{A}_{yy} = \mathcal{A}_{xy}$, the noises that drive the master and slave dynamics are exactly the same, i.e., equation (8) with $\xi_x(t) = \xi_y(t)$. This property follows by diagonalizing the matrix of diffusion noise coefficients $\{\{\mathcal{A}_{xx}, \mathcal{A}_{xy}\}, \{\mathcal{A}_{xy}, \mathcal{A}_{yy}\}\}$.

As is well known, in the absence of the external noises $\xi_x(t)$ and $\xi_y(t)$, the master–slave dynamics equation (8), after a time transient of order $1/\gamma$, reach the synchronized manifold $x(t+T) = y(t)$. Therefore, the slave variable *anticipates* the behavior of the master variable. The achievement of this state is clearly affected by the presence of the external noises. The degree of departure with respect to the perfectly synchronized manifold can be measured with a *similarity function*, defined as [49]

$$S(\tau) \equiv \lim_{t\to\infty} \left[\frac{\overline{\langle [x(t+\tau) - y(t)]^2 \rangle}}{[\overline{\langle x^2(t) \rangle}\, \overline{\langle y^2(t) \rangle}]^{1/2}} \right]^{1/2}. \tag{10}$$

As before, the overbar denotes an average with respect to the system initialization or equivalently a time average in the asymptotic regime. In the absence of the external noises, this object satisfies $S(T) = 0$, indicating that the perfectly synchronized state $x(t+T) = y(t)$ was achieved. In the presence of the noises, we expect $S(T) > 0$.

The characterization of the behavior of the similarity function $S(\tau)$ from the evolution equation (8) is in principle *a highly non-trivial task*. The major complication come from the chaotic nature of the master and slave dynamics. Even in the absence of the external noises, in general it is impossible to get an analytical expression for the similarity function. Nevertheless, if both dynamics are in the fully-developed chaos regime, from the previous section, we know that a simpler representation may be achieved. The Langevin approach to equation (8) reads

$$\dot{x}(t) = -\gamma x(t) + \eta(t-T) + \xi_x(t), \tag{11a}$$

$$\dot{y}(t) = -\gamma y(t) + \eta(t) + \xi_y(t). \tag{11b}$$

Note that this equation corresponds to equation (8) with the replacement $f[x] \to \eta$ and maintaining the respective time arguments. As before, the effective noise $\eta(t)$ is defined by the correlation equation (6). Furthermore, we will assume that $\overline{\eta(t)} = 0$. We will deal the case, $\overline{\eta(t)} \neq 0$ at the end of this section.

While the nature of equations (11) is completely different to that of equations (8), in the asymptotic time regime these Langevin equations, without the external noises $\xi_x(t)$ and $\xi_y(t)$, also reach a perfectly synchronized state. In fact, without the external noises, from equation (11) it is possible to write $(\mathrm{d}/\mathrm{d}t)[x(t) - y(t-T)] = -\gamma[x(t) - y(t-T)]$, implying that after a time transient of order $(1/\gamma)$ the manifold $x(t+T) = y(t)$ is reached. From the previous section we know that the statistical properties of the corresponding master process equations (8*a*) and (11*a*) are the same. Then, we estimate the similarity function equation (10) associated with the nonlinear evolution equation (8) from the simpler linear Langevin evolutions equation (11).

In the long-time limit ($\gamma t \gg 1$), the master and slave Langevin evolutions can be integrated for each realization of the noise $\eta(t)$, which represent the nonlinear force, and external noises $[\xi_x(t)$ and $\xi_y(t)]$ as $x(t) \approx \int_0^t \mathrm{d}t'\, \mathrm{e}^{-\gamma(t-t')}[\eta(t'-T) + \xi_x(t')]$, and as $y(t) \approx \int_0^t \mathrm{d}t'\, \mathrm{e}^{-\gamma(t-t')}[\eta(t') + \xi_y(t')]$, respectively. By using the correlation equations (6) (with $\overline{\eta(t)} = 0$) and (9), it follows

$$\lim_{t\to\infty} \overline{\langle x^2(t)\rangle} = \frac{\mathcal{A} + \mathcal{A}_{xx}}{2\gamma}, \qquad \lim_{t\to\infty} \overline{\langle y^2(t)\rangle} = \frac{\mathcal{A} + \mathcal{A}_{yy}}{2\gamma}. \tag{12}$$

In a similar way, we get

$$\lim_{t\to\infty} \overline{\langle x(t+\tau)y(t)\rangle} = \frac{\mathcal{A}}{2\gamma}\exp[-\gamma|\tau - T|] + \frac{\mathcal{A}_{xy}}{2\gamma}\exp[-\gamma|\tau|].$$

Therefore, the similarity function reads

$$S(\tau) = \sqrt{2}\left[\frac{\left(1 + \frac{\mathcal{A}_{xx}+\mathcal{A}_{yy}}{2\mathcal{A}}\right) - \left(\mathrm{e}^{-\gamma|\tau-T|} + \frac{\mathcal{A}_{xy}}{\mathcal{A}}\,\mathrm{e}^{-\gamma|\tau|}\right)}{\left(1 + \frac{\mathcal{A}_{xx}}{\mathcal{A}}\right)^{1/2}\left(1 + \frac{\mathcal{A}_{yy}}{\mathcal{A}}\right)^{1/2}}\right]^{1/2}. \tag{13}$$

This is one of the main results of this section. Note that this expression only depends on one free parameter, i.e., the amplitude of the chaotic force $\mathcal{A}$. On the other hand, this result relies in assuming the absence of any statistical correlation between the noise $\eta(t)$ representing the chaotic force and the external noises $\{\xi_x(t), \xi_y(t)\}$. Consistently with the delta correlated nature of both contributions, equations (6) and (9), we have also calculated the extra contributions to equation (13) that appear by assuming a delta cross correlation between both kinds of objects. Nevertheless, the numerical simulations presented along the paper contradict the existence of any extra correlation, supporting the (previous) arguments that explain the statistical independence between the chaotic force and any external source, equation (7).

From equation (13) one can analyze different limits. In the absence of external noise we get

$$S(\tau) = \sqrt{2}(1 - \exp[-\gamma|\tau - T|])^{1/2}. \tag{14}$$

Note that this expression does not depend on the chaotic force amplitude $\mathcal{A}$, it is defined only in terms of the local dissipation rate γ and the delay T. Consistently, $S(\tau)$ satisfies the anticipated synchronization condition $S(T) = 0$. When the external noise sources are taken in account, we get

$$S(T) = \sqrt{2}\left[\frac{\frac{\mathcal{A}_{xx}+\mathcal{A}_{yy}}{2\mathcal{A}} - \frac{\mathcal{A}_{xy}}{\mathcal{A}}\,\mathrm{e}^{-\gamma T}}{\left(1 + \frac{\mathcal{A}_{xx}}{\mathcal{A}}\right)^{1/2}\left(1 + \frac{\mathcal{A}_{yy}}{\mathcal{A}}\right)^{1/2}}\right]^{1/2}. \tag{15}$$

This value measures the departure with respect to the perfectly synchronized manifold $x(t+T) = y(t)$. Note that the correlation $\mathcal{A}_{xy}$ always decrease the value of $S(T)$. This effect is exponentially diminished when increasing γT.

3.1. Anticipated synchronization of delay maps

The previous results can be extended to the case of anticipated synchronization in discrete delay maps. We consider the maps that follow after discretizing the time variable in equation (8), $t = n\delta t$, and integrating both the master and slave evolutions up to first order in the discrete time step δt. We get

$$x_{n+1} = ax_n + bf(x_{n-n_0}) + \xi_n^x, \tag{16a}$$

$$y_{n+1} = ay_n + bf(x_n) + \xi_n^y. \tag{16b}$$

Here, n_0 defines the characteristic delay step and the 'dissipative' rate satisfies $0 < a < 1$. For each n, ξ_n^x and ξ_n^y, are independent Gaussian distributed variables with $\langle \xi_n^z \xi_m^{z'} \rangle = A_{zz'}\delta_{nm}$, $(z = x, y)$, subject to the constraint $A_{xx}A_{yy} - A_{xy}A_{yx} \geqslant 0$, $(A_{xy} = A_{yx})$ [50]. The parameters of the continuous time evolution equation (8) and the discrete map equation (16) are related by

$$\gamma = \frac{1-a}{\delta t}, \qquad \beta = \frac{b}{\delta t}, \qquad T = n_0\delta t, \qquad \mathcal{A}_{zz'} = \frac{A_{zz'}}{\delta t}. \tag{17}$$

For the discrete map, the similarity function equation (10) is defined as

$$S_m = \lim_{n\to\infty} \left[\frac{\overline{\langle (x_{n+m} - y_n)^2 \rangle}}{\sqrt{\langle \overline{x_n^2} \rangle \langle \overline{y_n^2} \rangle}} \right]^{1/2}. \tag{18}$$

As we will show in the next examples, this object can be fitted by equation (13) with the mapping equation (17). This property is valid when the discrete map provides a good approximation to the continuous time evolution. In fact, when $a \approx 1$, i.e., $\gamma\delta t \ll 1$, the map equation (16) can be read as a numerical algorithm for simulating the continuous time evolution equation (11). Nevertheless, we remark that equation (16) can also be analyzed without appealing to the parameter mapping equation (17), i.e., the Langevin approach can also be formulated for discrete time dynamic. S_m can be estimated after replacing the chaotic force in equation (16) by a discrete noise, $f(x) \to \eta_n$, with $\overline{\eta_n} = 0$ and $\overline{\eta_n \eta_m} = A\delta_{nm}$. We get

$$\lim_{n\to\infty} \langle \overline{x_n^2} \rangle = \frac{A + A_{xx}}{1-a^2}, \qquad \lim_{n\to\infty} \langle \overline{y_n^2} \rangle = \frac{A + A_{yy}}{1-a^2}. \tag{19}$$

The master–slave correlation reads

$$\lim_{n\to\infty} \langle \overline{(x_{n+m} y_n)} \rangle = \frac{1}{1-a^2}(Aa^{|m-no|} + A_{xy}a^{|m|}). \tag{20}$$

Then, the (discrete) similarity function reads

$$S_m = \sqrt{2}\left[\frac{\left(1 + \frac{A_{xx}+A_{yy}}{2A}\right) - \left(a^{|m-no|} + \frac{A_{xy}}{A}a^{|m|}\right)}{\left(1 + \frac{A_{xx}}{A}\right)^{1/2}\left(1 + \frac{A_{yy}}{A}\right)^{1/2}} \right]^{1/2}. \tag{21}$$

Consistently, by using equation (17) and the mapping between the chaotic force amplitudes

$$\mathcal{A} = A\delta t^{-1}, \tag{22}$$

from equation (21) to first order in δt, one recovers equation (13). Furthermore, the conditions that guarantee the validity of the Langevin representation in the continuous time case, i.e., $\beta T \gg 1$ and $\gamma/\beta \ll 1$, from the mapping equations (17), here read $bn_0 \gg 1$ and $(1-a)/b \ll 1$.

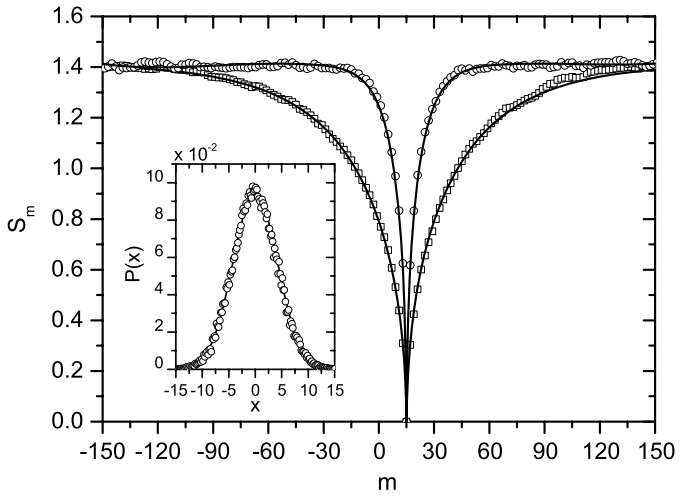

Figure 1. Similarity function of the coupled delay maps equation (23) without noise, $A_{xx} = A_{yy} = A_{xy} = 0$. The parameters are $n_0 = 15, b = 3$, and $a = 0.975$ (squares) and $a = 0.9$ (circles). The lines correspond to the fitting equation (14) joint with the mapping equation (17) (with $\delta t = 1$) indistinguishable from equation (21). The inset corresponds to the stationary probability distribution $P(x)$ of the process x_n (with $a = 0.9$).

3.2. Numerical results

To check the validity of the previous results, we consider an Ikeda-like delay-differential equation [18, 19], i.e. equation (8) with $f[x] = \sin(x)$. Its associated discrete map (equation (16)) read

$$x_{n+1} = ax_n + b\sin(x_{n-n_0}) + \xi_n^x, \tag{23a}$$

$$y_{n+1} = ay_n + b\sin(x_n) + \xi_n^y. \tag{23b}$$

To obtain the following results, we generate a set of realizations from the map equation (23) by considering different random initials conditions in the interval $(-\pi, \pi)$ for both, the master and the slave variables. By averaging over this set of realizations ($\approx 10^4$), we determine numerically the similarity function equation (18). To check the ergodic property of the corresponding chaotic attractor, we repeated the numerical calculations by averaging over time a single trajectory with an arbitrary set of initial conditions. Consistently, we obtained the same results and characteristic behaviors.

In figure 1 we show the similarity function when the external noises are absent, i.e., the similarity corresponding to the deterministic map. In agreement with this condition, we note that $S_{n_0} = 0$, implying that the manifold $x_{m+n_0} = y_m$ characterizes the asymptotic behavior. Furthermore, we find that both the expressions for the continuous time case (equation (13) with the mapping equation (17)), as well as the similarity function of the map (equation (21)) are indistinguishable from each other (in the scale of the graphic) and both correctly fit the numerical behavior. In the inset, we show the stationary probability distribution of the master process x_n. In agreement with our considerations, this distribution can be fit with a Gaussian distribution. From its width, and by using equation (19) (or equation (12)) we estimated the value of the chaotic force amplitude, $A \approx 3.5$.

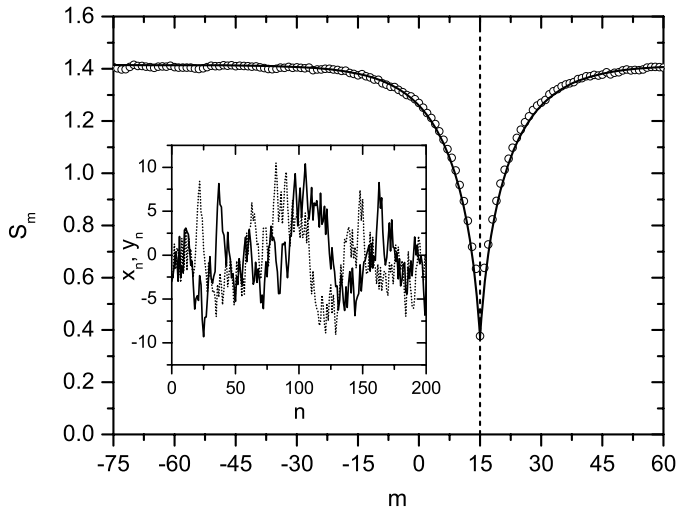

Figure 2. Similarity function of the coupled delay maps equation (23) subject to external Gaussian noise fluctuations. The parameters are $n_0 = 15, a = 0.9$ and $b = 3$. The noise parameters are $A_{xx} = A_{yy} = 0.25$ and $A_{xy} = 0$. The line corresponds to the fitting equation (14) joint with the mapping equation (17) (with $\delta t = 1$) indistinguishable from equation (21). The chaotic noise amplitude results $A \approx 3.5$. The inset corresponds to a master (x_n, full line) and slave (y_n, dotted line) realizations.

In the absence of the noises, we corroborate that by taking the function $f[x] = \sin(x+\phi)$, independently of the value of the phase ϕ, the same statistical behaviors follow. This result confirms the arguments presented in the previous section (equation (2)) about the statistical invariance of the chaotic force under a shift of its argument.

In figure 2 we show the similarity function when the master and slave dynamics are affected by two uncorrelated external noises. As expected, we found that $S_{n_0} > 0\,(n_0 = 15)$. In the inset, we show a characteristic master–slave realization. Even in the presence of the external noises, both trajectories are approximately the same (the slave anticipate the master trajectory). In contrast with the previous figure, here the fitting to the similarity function depends explicitly on the chaotic force amplitude A. We found that the value of A that provides the best fitting is consistent with that found for the deterministic map (figure 1), i.e., $A \approx 3.5$. Then, in this case, the inequality $A \gg \{A_{xx}, A_{yy}\}$ is satisfied, implying that the fluctuations induced by the determinist chaotic dynamic are much larger than those induced by the external noise sources.

Maintaining all the parameter values corresponding to figure 2, we analyzed the case $A_{xx} = A_{yy} = A_{xy}$. In this situation, the noises that drive the master and slave dynamics are exactly the same, i.e., equation (23) with $\xi_n^x = \xi_n^y$ (as in the continuous time case, this property follows by diagonalizing the matrix of diffusion noise coefficients $\{\{A_{xx}, A_{xy}\}, \{A_{xy}, A_{yy}\}\}$). We found that the similarity function is almost indistinguishable from that of figure 2. Independently of the external noise correlations, in both cases our approach provides a very good fitting of the numerical results.

In figure 3, by maintaining the parameters of the deterministic map, i.e., (a, b, n_0), we increased the amplitude of the external noises, such that $\{A_{xx}, A_{yy}\} \approx A$. Then, the external noise-induced fluctuations are of the same order as the intrinsic chaotic dynamical fluctuations. Even in this limit, our approach provides an excellent fitting of the numerical results. Both, the case of uncorrelated noises ($A_{xy} = 0$ with $A_{xx} = A_{yy}$) and the case of completely

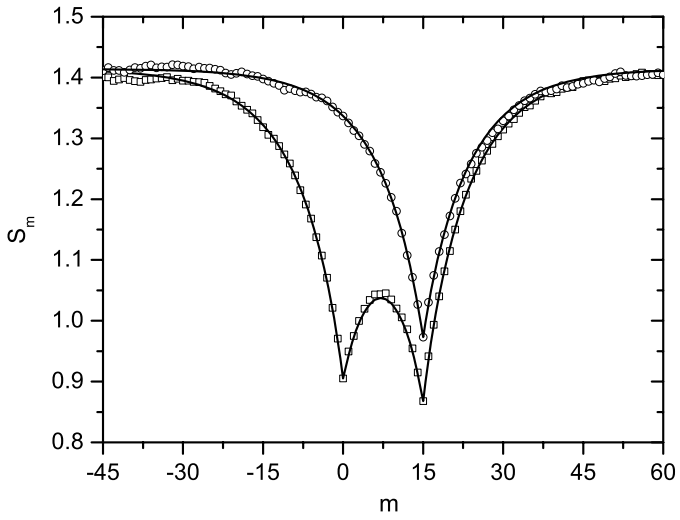

Figure 3. Similarity function of the coupled delay maps equation (23) driven by different noises. The circles correspond to $A_{xx} = A_{yy} = 3.5$ and $A_{xy} = 0$, while the squares correspond to $A_{xx} = A_{yy} = A_{xy} = 3.5$. The parameters of the map are the same as in figure 2. The lines correspond to the fitting equation (14) joint with the mapping equation (17) (with $\delta t = 1$) indistinguishable from equation (21). The chaotic noise amplitude results $A \approx 4.3$.

correlated noises ($A_{xx} = A_{yy} = A_{xy}$) are considered. In both situations, since the external noise amplitudes are larger than in figure 2, the value of S_{n_0} increases, indicating a weaker (anticipated) synchronization between the master and slave dynamics.

In the case of completely correlated noises, $A_{xx} = A_{yy} = A_{xy}$, the similarity function develops two (local) minima, one at $m = n_0$ and other at $m = 0$. This feature follows from the competition between two different synchronizing mechanisms, induced by the chaotic dynamics and the external noises, respectively. In fact, as the noise that drives the master and slave dynamics is the same, its action tends to synchronize both dynamics without any time shift (see equation (23) with $\xi_n^x = \xi_n^y$), producing the dip at $m = 0$. In agreement with this argument, from equation (21) (or equivalently equation (13)) one can deduce that only one minimum at $m = 0$ will be appreciable in the similarity function when $A \ll A_{xx} = A_{yy} = A_{xy}$, i.e., in the limit of high-noise intensity.

As in figure 2, the similarity function depends on the amplitude A of the chaotic force. Here, the best fitting to the similarity function is obtained with $A \approx 4.3$. This value is larger than those associated with the deterministic dynamics (figure 1) or the case of weak external noises (figure 2). Then, in general it is necessary to consider that the chaotic force amplitude A is also a function of the external noise intensities, $A = A[\{f(x), b\}, A_{xx}, A_{yy})]$. We remark that in concordance with the Langevin representation, the value of A determined from equations (19)–(21) is the same. By using the parameters of figure 3, we found a moderate dependence on the external noise intensities, i.e., the maximal variation of A with the amplitude of the noises does not exceed 30% of the deterministic map value (figure 1, $A \approx 3.5$). The dependence is smooth but non-monotonous. We found that A saturates to a fixed value ($A \approx 4.5$) when increasing the external noise amplitudes, $A < \{A_{xx}, A_{yy}\}$.

3.3. Chaotic force with a non-null average value

Our previous theoretical calculations rely on the assumption that the average (over realizations or its stationary time average) of the chaotic force is zero, i.e., $\overline{f[x(t)]} = 0$.

When the dynamic, that does not include the nonlinear contribution, is purely dissipative (equation (1) with $f(x) \to 0$,) the validity of this assumption requires that $f(x)$ takes symmetrically positive and negative values. Functions that do not satisfy this property also arise in real experimental setups [21, 26, 43]. In these cases, due to the pure dissipative nature of the evolution equation (8) (or equation (16)), in the long-time limit the master–slave realizations will fluctuate around a non-null fixed value.

This situation can be managed by writing $f(x) = [f(x) - \overline{f(x)}] + \overline{f(x)}$. Then, the previous theoretical calculations can be easily extended by replacing $[f(x) - \overline{f(x)}] \to \eta(t)$ (with $\overline{\eta(t)} = 0$) and by maintaining the extra contribution $\overline{f(x)}$ in the final Langevin representation. For example, taking the functions $f(x) = \sin^2(x)$ or $f(x) = \cos^2(x)$ in equation (8), from the Langevin representation equation (11), it is possible to deduce that in the fully-developed chaos regime the master–slave realizations will fluctuate around $\beta/(2\gamma)$.

When the dynamic without the nonlinear contribution can by itself induce symmetric dynamical oscillations, the symmetry requirement on the function $f(x)$ may be eliminated (see section 5).

4. Effect of parameters mismatch in a hyperchaotic communication scheme

Hyperchaotic delay dynamics may be used as a resource for secure encoded communication. Different schemes have been proposed, in all the cases, it is argued that the security of the communication channel may be improved by increasing the dimension of the hyperchaotic attractor. Here, we study the dynamics [26]

$$\dot{x}(t) = -\gamma x(t) + \beta f[x(t-T)] + \mathfrak{M}(t), \tag{24a}$$

$$\dot{y}(t) = -\gamma' y(t) + \beta' f[x(t-T')]. \tag{24b}$$

The variable $x(t)$ is the carrier signal where the message is encoded. The external feed $\mathfrak{M}(t)$ is defined by $\mathfrak{M}(t) = [\mathrm{d}\mathfrak{m}(t)/\mathrm{d}t + \gamma \mathfrak{m}(t)]$, where $\mathfrak{m}(t)$ is the message to be transmitted. The variable $y(t)$ is the receiver. It is easy to demonstrate that in the stationary regime the state $x(t) - y(t) = \mathfrak{m}(t)$ is reached, implying that the receiver is able to unmask the message encoded in the hyperchaotic dynamics of $x(t)$. This condition is only satisfied when the characteristic parameters of the transmitter and receiver evolutions (equation (24)) are the same, i.e., $\gamma' = \gamma, \beta' = \beta$ and $T' = T$.[3] In any real experimental situation, it is expected that this condition is not fulfilled, i.e., the decodification of the message is performed in the presence of an unavoidable (finite) parameter mismatching. For simplicity, in the present section we will not consider the action of any external noise perturbation source.

In order to achieve a general characterization of the influence of the parameters mismatch, we take $\mathfrak{M}(t) = 0$. As in the previous section, we will use the similarity function $S(\tau)$ (equation (10)) as a measure of the degree of synchronization between the emitter and receiver variables.

When the transmitter dynamics is in the fully-developed chaos regime, we can extend the Langevin approach to the present situation. In order to estimate the similarity function, we replace the chaotic coupled evolution equation (24) by the Langevin equations

$$\dot{x}(t) = -\gamma x(t) + \eta(t-T), \tag{25a}$$

[3] It is also possible to consider extra parameters mismatch in the transmitter–receiver nonlinearities, as for example the phase ϕ in $f(x) = \sin(x + \phi)$ [43]. This case can be worked out in the Langevin representation in a similar way by discomposing the sin function in two shiftless terms and considering their respective symmetries properties. For simplicity, we will not consider this case.

$$\dot{y}(t) = -\gamma' y(t) + \sqrt{\alpha}\eta(t - T'), \tag{25b}$$

where the parameter α is defined by

$$\alpha \equiv \left(\frac{\beta'}{\beta}\right)^2. \tag{26}$$

As before, the noise $\eta(t)$ is characterized by $\overline{\eta(t)} = 0$ and $\overline{\eta(t)\eta(t')} = \mathcal{A}\delta(t - t')$ (equation (6)). The similarity function $S(\tau)$ associated with equation (25), can be determine analytically by a straightforward calculation. We get

$$S(\tau) = \left[\sqrt{\frac{\gamma'}{\alpha\gamma}} + \sqrt{\frac{\alpha\gamma}{\gamma'}} - \frac{4\sqrt{\gamma\gamma'}}{(\gamma + \gamma')}\exp[-\bar{\gamma}|\tau - \Delta|]\right]^{1/2}, \tag{27}$$

where we have defined the delay time mismatch

$$\Delta \equiv T - T', \tag{28}$$

and the rate $\bar{\gamma}$ is defined as

$$\bar{\gamma} \equiv \begin{cases} \gamma & \text{for} \quad \tau > \Delta \\ \gamma' & \text{for} \quad \tau < \Delta. \end{cases} \tag{29}$$

We note that due to the normalization constants in the definition of the similarity function equation (10), the final expression equation (27) does not depend explicitly on the chaotic force amplitude $\mathcal{A}$. The similarity function only satisfies $S(0) = 0$, when the transmitter–receiver parameters are exactly the same. In this situation, the manifold $x(t) = y(t)$ characterizes the stationary regime.

4.1. Parameter mismatch in discrete delay maps

The previous results can be extended to the coupled maps obtained from the evolution equation (24) after a first-order Euler integration, i.e.,

$$x_{n+1} = a x_n + b f\left(x_{n-n_0}\right), \tag{30a}$$

$$y_{n+1} = a' y_n + b' f\left(x_{n-n_0'}\right). \tag{30b}$$

Here, the transmitter and receiver parameters of both, the continuous and the discrete time evolutions, must be related as

$$\gamma = \frac{1-a}{\delta t}, \qquad \beta = \frac{b}{\delta t}, \qquad T = n_0 \delta t, \tag{31a}$$

$$\gamma' = \frac{1-a'}{\delta t}, \qquad \beta' = \frac{b'}{\delta t}, \qquad T' = n_0' \delta t, \tag{31b}$$

where δt is the characteristic discretization time step. For the discrete maps, the similarity function equation (18) reads

$$S_m = \left[\sqrt{\frac{(1-a'^2)}{\alpha(1-a^2)}} + \sqrt{\frac{\alpha(1-a^2)}{(1-a'^2)}} - \frac{2\sqrt{(1-a^2)(1-a'^2)}}{(1-aa')}\bar{a}^{|m-m_0|}\right]^{1/2}, \tag{32}$$

where we have defined

$$m_0 \equiv n_0 - n_0', \qquad \alpha = \left(\frac{b'}{b}\right)^2, \tag{33}$$

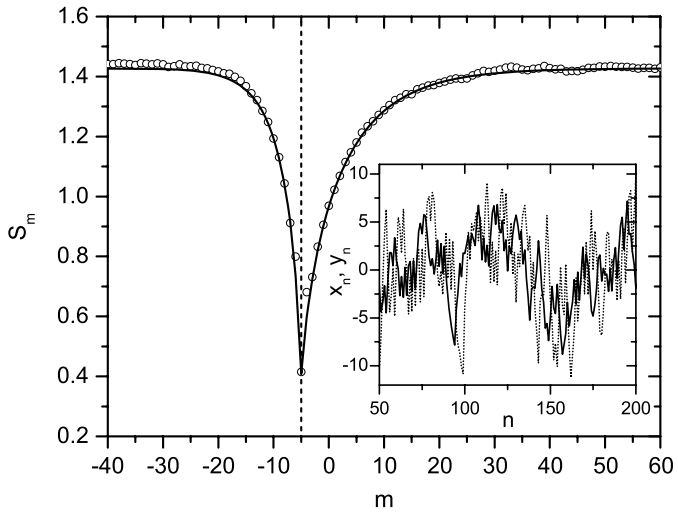

Figure 4. Similarity function of the coupled delay maps equation (35) (circles). The parameters are $n_0 = 15, a = 0.9, b = 3$ and $n_0' = 20, a' = 0.8, b' = 5$. The line corresponds to the fitting equation (27) joint with the mapping equation (31) (with $\delta t = 1$), indistinguishable from equation (32). The inset corresponds to a realization of x_n (full line), and y_n (dotted line).

and the 'dissipative rate'

$$\bar{a} \equiv \begin{cases} a & \text{for} \quad m > m_0 \\ a' & \text{for} \quad m < m_0. \end{cases} \tag{34}$$

Note that under the mapping equation (31), the definition of the parameter α in equation (33) is consistent with equation (26).

4.2. Numerical results

Here we consider the coupled chaotic maps

$$x_{n+1} = a x_n + b \cos\left(x_{n-n_0}\right), \tag{35a}$$

$$y_{n+1} = a' y_n + b' \cos\left(x_{n-n_0'}\right). \tag{35b}$$

In the inset of figure 4, we show a characteristic realization of the emitter and receiver variables. By averaging over different realizations ($\approx 10^4$), we get the similarity function. We note that due to the specific values of the characteristic parameters, the receiver 'synchronizes' with the 'past' of the transmitter variable. In fact, S_m attains its minimal value at $m_0 = -5$. Furthermore, due to the difference in the parameters b and b', the amplitude of the receiver fluctuations are bigger than those of the transmitter.

In contrast with figure 2, here the similarity function is not symmetrical around its minimal value. This asymmetry has its origin in the mismatch between the 'dissipative rate' parameters a and a'.

Clearly, the Langevin approach provides a very well fitting to the numerical simulations. Furthermore, it allows us to characterize the influence of the parameters mismatch on the synchronization of the transmitter and receiver variables. The analytical quantification of this

effect can be obtained from the similarity function equation (27) (or equation (32)) evaluated at the origin

$$S(0) = \left[\sqrt{\frac{\gamma'}{\alpha\gamma}} + \sqrt{\frac{\alpha\gamma}{\gamma'}} - \frac{4\sqrt{\gamma\gamma'}}{(\gamma+\gamma')}\exp[-\bar{\gamma}|\Delta|]\right]^{1/2}. \tag{36}$$

By a direct inspection of this expression, we realize that the dependence of $S(0)$ on the prime parameters is non-monotonous, $S(0)$ develops different minima when varying the receiver parameters. In agreement with the results of [43], assuming that it is possible to adjust a given receiver parameter, the previous expression allows us to choose the best value that maximizes the synchronization phenomenon.

5. Synchronization of second-order nonlinear delay differential equations

In the previous sections, we analyzed the phenomenon of chaotic synchronization for dynamics generated by first-order delay equations. Nevertheless, second-order delay differential equations also arise in the description of real experimental setups. By second order we mean equations whose linear dynamical contributions are equivalent to second-order (time) derivative evolutions. Here, we demonstrate that the Langevin approach also works in that case.

Following [43] we consider the evolution

$$x(t) + \frac{\dot{x}(t)}{\gamma} + \frac{1}{\theta}\int_0^t x(s)\,\mathrm{d}s = \beta\cos^2[x(t-T)] + \xi_x(t), \tag{37}$$

$$y(t) + \frac{\dot{y}(t)}{\gamma'} + \frac{1}{\theta'}\int_0^t y(s)\,\mathrm{d}s = \beta'\cos^2[x(t-T')] + \xi_y(t), \tag{38}$$

which describe synchronization in a set of coupled *electro-optical laser devices*. The integral contributions proportional to $(1/\theta)$ and $(1/\theta')$ indicate that the linear evolutions defined by the left-hand side of equations (37) and (38) are equivalent to a set of second-order derivative differential equations. In addition to the parameters mismatch, we also consider the action of external additive noises $\xi_x(t)$ and $\xi_y(t)$, whose mutual and self-correlations are defined by equation (9). In order to simplify the final expression here we do not consider any mismatch in the phase of the chaotic forces (see footnote 3).

Under the same conditions than in the previous sections, we assume that $x(t)$ and $y(t)$, in the long-time limit, attain the fully-developed chaos regime, allowing us to replace the nonlinear delay forces by noise contributions with the same time arguments, delivering

$$x(t) + \frac{\dot{x}(t)}{\gamma} + \frac{1}{\theta}\int_0^t x(s)\,\mathrm{d}s = \eta(t-T) + \xi_x(t), \tag{39a}$$

$$y(t) + \frac{\dot{y}(t)}{\gamma'} + \frac{1}{\theta'}\int_0^t y(s)\,\mathrm{d}s = \sqrt{\alpha}\eta(t-T') + \xi_y(t), \tag{39b}$$

where as before, $\alpha = (\beta'/\beta)^2$. The correlation of $\eta(t)$ is again defined by equation (6), and we take $\overline{\eta(t)} = 0$. Note that in spite that the nonlinear contribution $\cos^2[x]$ is always positive, when $\{\theta, \theta'\} < \infty$, the second-order linear evolution introduces self-dynamical oscillations that imply that its effective action averaged over realizations (or its stationary time average) must be taken as zero. This property breaks down when the integral contributions are absent, i.e., in the limit $\theta = \theta' = \infty$.

The Green's functions associated with the linear evolutions equation (39) can be obtained straightforwardly in the Laplace domain, being defined by the addition of two exponential functions. After integrating formally both equations for each realization of the noises, it follows

$$\lim_{t\to\infty}\langle\overline{x^2(t)}\rangle = \frac{\gamma}{2}(\mathcal{A}+\mathcal{A}_{xx}), \tag{40a}$$

$$\lim_{t\to\infty}\langle\overline{y^2(t)}\rangle = \frac{\gamma'}{2}(\alpha\mathcal{A}+\mathcal{A}_{yy}). \tag{40b}$$

The similarity function (equation (10)) reads

$$S(\tau) = \left\{ \frac{\sqrt{\frac{\gamma}{\alpha\gamma'}}\left(1+\frac{\mathcal{A}_{xx}}{\mathcal{A}}\right)+\sqrt{\frac{\alpha\gamma'}{\gamma}}\left(1+\frac{\mathcal{A}_{yy}}{\alpha\mathcal{A}}\right)-4\mu\left[\Xi(\tau-\Delta)+\frac{\mathcal{A}_{xy}}{\sqrt{\alpha}\mathcal{A}}\Xi(\tau)\right]}{\left(1+\frac{\mathcal{A}_{xx}}{\mathcal{A}}\right)^{1/2}\left(1+\frac{\mathcal{A}_{yy}}{\alpha\mathcal{A}}\right)^{1/2}} \right\}^{1/2}. \tag{41}$$

Here, $\Delta = T - T'$. The function $\Xi(t)$ is defined as

$$\Xi(t) = \mathrm{e}^{-\frac{1}{2}\bar{\gamma}|t|}\left[\cosh(\bar{\Phi}|t|/2) - \bar{\nu}\frac{\bar{\gamma}}{\bar{\Phi}}\sinh(\bar{\Phi}|t|/2)\right], \tag{42}$$

where the dissipative rate $\bar{\gamma}$ is defined by

$$\bar{\gamma} \equiv \begin{cases} \gamma & \text{if} \quad t > 0 \\ \gamma' & \text{if} \quad t < 0. \end{cases} \tag{43}$$

For $t > 0$, the frequency $\bar{\Phi}$ reads

$$\bar{\Phi} \equiv \gamma\sqrt{1-\frac{4}{\theta\gamma}}, \qquad \text{if} \quad t > 0, \tag{44}$$

while the dimensionless parameter $\bar{\nu}$ is

$$\bar{\nu} \equiv 1 - \frac{2}{\theta(\theta+\theta')}\left(\frac{\theta}{\gamma}-\frac{\theta'}{\gamma'}\right), \qquad \text{if} \quad t > 0. \tag{45}$$

For $t < 0$, both Φ and ν are defined by interchanging $\theta \leftrightarrow \theta'$ and $\gamma \leftrightarrow \gamma'$ in the previous expressions. Finally, in equation (41), we have also defined the dimensionless parameter

$$\mu \equiv \frac{\sqrt{\gamma\gamma'}(\theta+\theta')}{(\theta\gamma'/\theta'\gamma)+[(\theta+\theta')(\gamma+\gamma')-2]+(\theta'\gamma/\gamma'\theta)}, \tag{46}$$

which is symmetric in the emitter and receiver parameters.

In order to check the validity of the previous approach, we consider the discrete maps associated with equations (37) and (38) by Euler integration

$$x_{n+1} = ax_n - \omega\sum_{j=0}^{n}x_j + b\cos^2\left(x_{n-n_0}\right) + \xi_n^x, \tag{47a}$$

$$y_{n+1} = a'y_n - \omega'\sum_{j=0}^{n}y_j + b'\cos^2\left(x_{n-n_0'}\right) + \xi_n^y. \tag{47b}$$

The (transmitter) parameters mapping reads

$$\gamma = \frac{(1-a)}{\delta t}, \qquad \theta = \delta t\frac{(1-a)}{\omega}, \qquad \beta = \frac{b}{(1-a)}. \tag{48}$$

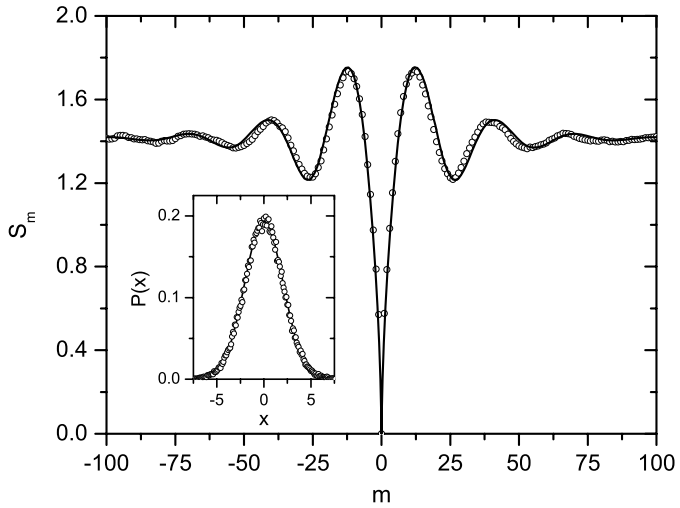

Figure 5. Similarity function of the coupled delay maps equation (47) (circles) without noises, $A_{xx} = A_{yy} = A_{xy} = 0$ and without mismatching, $n_0' = n_0, a' = a, b' = b$ and $\omega' = \omega$. The parameters are $n_0 = 20, a = 0.9, b = 3$ and $\omega = 0.05$. The line corresponds to the fitting equation (41) under the mapping equation (48) (with $\delta t = 1$). The inset corresponds to the stationary probability distribution of the process x_n.

The same relations are valid for the prime (receiver) parameters. The noises ξ_n^x and ξ_n^y, joint with the corresponding mapping for their amplitudes are defined below equation (16). The chaotic force amplitude of the continuous and discrete time evolutions are related by $\mathcal{A} = A/\delta t$.

In figure 5 we plot the similarity function (equation (18)) associated with the coupled maps equation (47) in the absence of parameters mismatch and without the external noises. The analytical result equation (41), under the mapping equation (48), provides an excellent fitting of the numerical results. In contrast with the previous sections (see for example figure 1), here the similarity function develops an oscillatory behavior, its origin can be associated with the integral contributions in the dissipative dynamics of equations (37) and (38). Their characteristic frequency follows from equation (44).

In order to check the achievement of the fully-developed chaos regime[4], in the inset we show the stationary probability distribution of x_n. Consistently, this distribution can be fitted with a Gaussian distribution.

In figure 6, for other set of characteristic parameters, we plot the similarity function in the presence of parameter mismatch and external noise sources. As in the previous case, the fitting equation (41) correctly match the numerical results. The effective chaotic force amplitude is $A \approx 1.2$. The asymmetry of S_m around its minimum value follows from the parameter mismatch between the evolution of x_n and y_n.

[4] Taking the experimental parameters of [43], the dynamics goes beyond the Gaussian chaos regime. Our formalism may also be used as an estimator of the statistical properties in this regime. Nevertheless, the quality of the fitting departs from that showed in the figures of this paper. On the other hand, from equation (39), it is possible to write the Fourier transform ($t \to w$) of $x(t)$ as $x(w) = \{i\gamma w/[-w^2 + i\gamma w + \gamma/\theta)]\}[\eta(w) + \xi_x(w)]$, and a similar one for $y(w)$. Then, the band-pass filter approximation introduced in [43] can be read as a rough approximation to these expressions.

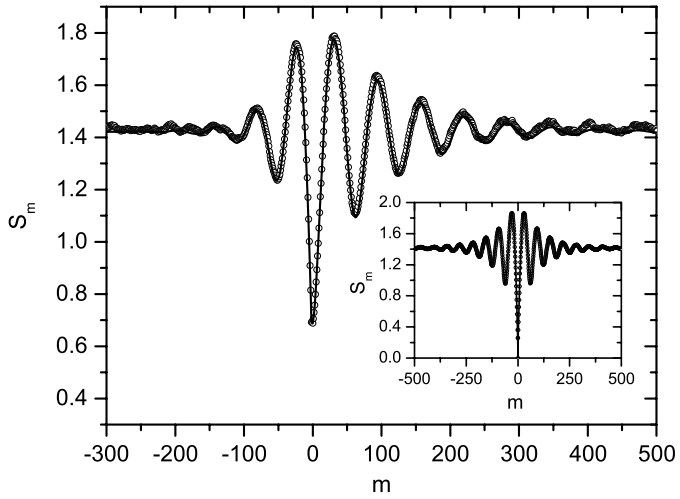

Figure 6. Similarity function of the coupled delay maps equation (47) (circles) with parameters mismatch and under the action of external noises. The parameters are $n_0 = 20, a = 0.98$, $b = 3, \omega = 0.01$, and $n_0' = 22, a' = 0.95, b' = 4, \omega' = 0.0125$. The noise parameters are $A_{xx} = A_{yy} = 0.0225$ and $A_{xy} = 0$. The line corresponds to the fitting equation (41) joint with the mapping equation (48) (with $\delta t = 1$). The inset corresponds to the similarity function in absence of noises and without mismatching.

In the inset, maintaining the parameters corresponding to the evolution of x_n, we plot the similarity function in the absence of both, parameters mismatch and the external noise contributions. In this case, the chaotic force amplitude (determine from equation (40)) is $A \approx 1$.

As in the previous section, a remarkable aspect of our analytical results is that they allow us to know the influence of different realistic effects on the chaotic synchronized manifold. For example, for a given set of fixed parameters, which may include the amplitude of the external noises, one can determine the value of the rest of the parameters that minimizes the similarity function at $\tau = 0$, giving rise to a maximization in the degree of synchronization between the emitter and receiver variables. This kind of analysis follows straightforwardly from our analytical results.

6. Conclusions

In this paper, we have characterized the phenomenon of chaotic synchronization in scalar-coupled nonlinear time delay dynamics. Our formalism relies in recognizing that in a fully-developed chaos regime, the trajectories associated with a broad class of hyperchaotic attractors are statistically equivalent to the realizations of a linear Langevin equation. This equivalence can be established when the function that defines the driven chaotic delay force is an oscillatory one, such that its dynamical action can be represented by a delta-correlated noise. Given this Langevin representation, the coupled nonlinear delay evolutions, where the phenomenon of chaotic synchronization happens, are replaced by a set of linear stochastic equations where the noise that represents the chaotic force maintains the corresponding time arguments. The statistical properties of the Langevin equations can be obtained analytically, providing an excellent estimation of the stationary statistical properties of the synchronized manifold.

Using the Langevin representation, we analyzed the phenomenon of anticipated synchronization in the presence of external additive noises. We also characterized the effect of parameters mismatch in a hyperchaotic communication scheme. Second-order delay equations associated with an electro optical device were also characterized. The analytical predictions of the Langevin approach correctly fit numerical simulations in discrete-coupled nonlinear delay maps associated with the corresponding continuous time evolutions.

In all cases, the degree of synchronization (between the master–slave or emitter–receiver variables) was characterized through a similarity function, defined in terms of the correlation between the synchronizing systems. When the departure from perfect synchronization is due to a parameter mismatching, the fitting to the similarity function does not involve any free parameter. When the action of external noises is considered the fitting depends on the effective chaotic force amplitude.

Our results are interesting from both, theoretical and experimental point of view. From our analytical expressions it is possible to evaluate under which conditions a given undesired effect can be minimized by controlling the rest of the parameters. On the other hand, in the context of hyperchaotic communication schemes, while high-dimensional systems increase the complexity of the masking signals, our results show that the corresponding statistical properties may adopt a simple analytical form. In fact, by measuring the similarity function our results allow us to infer the value of some of the characteristic parameters of the hyperchaotic delay dynamics.

The present study may be continued in different relevant directions such as the extension of the Langevin representation beyond the fully-developed chaos regime (non-Gaussian chaos) as well as for non-scalar chaotic dynamics. Furthermore, the characterization of the dependence of the effective chaotic force amplitude with the external noise parameters is an open interesting issue.

Acknowledgments

The author thanks fruitful discussions with Professor D H Zanette at Centro Atómico Bariloche, as well as with Professor G Buendia at Consortium of the Americas for Interdisciplinary Science. This work was mainly supported by CONICET, Argentina, and by Consortium of the Americas for Interdisciplinary Science, NSF's International Division via Grant INT-0336343.

References

[1] Pikovsky A, Rosenblum M and Kurths J 2001 *Synchronization, A Universal Concept in Nonlinear Sciences (Cambridge Nonlinear Science Series* vol 12*)* (Cambridge: Cambridge University Press)
[2] Fujisaka H and Yamada T 1983 *Prog. Theor. Phys.* **69** 32
Fujisaka H and Yamada T 1986 *Prog. Theor. Phys.* **75** 1087
[3] Pikovsky A S 1984 *Radiophys. Quantum Electron.* **27** 576
[4] Pikovsky A S 1985 *Sov. J. Commun. Technol. Electron* **30** 85
[5] Pikovsky A S and Grassberger P 1991 *J. Phys. A: Math. Gen.* **24** 4587
[6] Pecora L M and Carroll T L 1990 *Phys. Rev. Lett.* **64** 821
[7] Pecora L M and Carroll T L 1991 *Phys. Rev.* A **44** 2374
[8] Rossler O E 1979 *Phys. Lett.* A **71** 155
[9] Kocarev L and Parlitz L 1995 *Phys. Rev. Lett.* **74** 5028
[10] Peng J H, Ding E J, Ding M and Yang W 1996 *Phys. Rev. Lett.* **76** 904
[11] Lai Y C 1997 *Phys. Rev.* E **55** 4861
[12] Ali M K and Fang J Q 1997 *Phys. Rev.* E **55** 5285
[13] Short K M and Parker A T 1998 *Phys. Rev.* E **58** 1159
[14] Mackey M C and Glass L 1977 *Science* **197** 287

[15] Foss J, Longtin A, Mensour B and Milton J 1996 *Phys. Rev.* **76** 708
[16] MacDonald N 1989 *Biological Delay Systems: Linear Stability Theory* (Cambridge, England: Cambridge University Press)
[17] Asea P K and Zak P J 1999 *J. Econ. Dyn. Control* **23** 1155
Mackey M C 1989 *J. Econ. Theory* **48** 497
[18] Ikeda K, Daido H and Akimoto O 1980 *Phys. Rev. Lett.* **45** 709
[19] Ikeda K and Matsumoto K 1987 *Phys.* D **29** 223
[20] Arecchi F, Gadomski W and Meucci R 1993 *Phys. Rev.* A **34** 1617
[21] Larger L, Lacourt P A, Poinsot S and Hanna M 2005 *Phys. Rev. Lett.* **95** 043903
[22] Berre M Le, Ressayre E, Tallet A and Gibbs H M 1986 *Phys. Rev. Lett.* **56** 274
[23] Farmer J D 1982 *Physica* D **4** 366
[24] Grassberger P and Procaccia I 1983 *Physica* D **9** 189
[25] Berre M Le, Ressayre E, Tallet A, Gibbs H M, Kaplan D L and Rose M H 1987 *Phys. Rev.* A **35** 4020
[26] Goedgebuer J P, Larger L and Porte H 1998 *Phys. Rev. Lett.* **80** 2249
[27] Zhou C and Lai C H 1999 *Phys. Rev.* E **60** 320
[28] Yaowen L, Guangming G, Hong Z and Yinghai W 2000 *Phys. Rev.* E **62** 7898
[29] Udaltsov V S, Goedgebuer J P, Larger L and Rhodes W T 2001 *Phys. Rev. Lett.* **86** 1892
[30] Voss H U 2000 *Phys. Rev.* E **61** 5115
Voss H U 2000 *Phys. Rev.* E **64** 039904
[31] Voss H U 2001 *Phys. Rev. Lett.* **87** 014102
[32] Voss H U 2001 *Phys. Lett.* A **279** 207
[33] Pyragas K 1998 *Phys. Rev.* E **58** 3067
[34] Masoller C 2001 *Phys. Rev. Lett.* **86** 2782
[35] Masoller C and Zanette D H 2001 *Physica* A **300** 359
[36] Sivaprakasam S, Shahverdiev E M, Spencer P S and Shore K A 2001 *Phys. Rev. Lett.* **87** 154101
[37] Heil T, Fischer I, Elsässer W, Mulet J and Mirasso C R 2001 *Phys. Rev. Lett.* **86** 795
[38] Hernandez-Garcia E, Masoller C and Mirasso C R 2002 *Phys. Lett.* A **295** 39
[39] Ciszak M, Calvo O, Masoller C, Mirasso C R and Toral R 2003 *Phys. Rev. Lett.* **90** 204102
[40] Tang S and Liu J M 2003 *Phys. Rev. Lett.* **90** 194101
[41] Gauthier D J and Bienfang J C 1996 *Phys. Rev. Lett.* **77** 1751
[42] Johnson G A, Mar D J, Carroll T L and Pecora L M 1998 *Phys. Rev. Lett.* **80** 3956
[43] Kouomou Y C and Colet P 2004 *Phys. Rev.* E **69** 056226
[44] Brown R, Rulkov N F and Tufillaro N B 1994 *Phys. Rev.* E **50** 4488
[45] Lin W and He Y 2005 *Chaos* **15** 023705
[46] Györgyi G and Szépfalusy P 1983 *J. Stat. Phys.* **34** 451
[47] Dorizzi B, Grammaticos B, Berre M Le, Pomeau Y, Ressayre E and Tallet A 1987 *Phys. Rev.* A **35** 328
[48] Berre M Le, Ressayre E, Tallet A and Pomeau Y 1990 *Phys. Rev.* A **41** 6635
[49] Rosenblum M G, Pikovsky A S and Kurths J 1997 *Phys. Rev. Lett.* **78** 4193
[50] van Kampen N G 1992 *Stochastic Processes in Physics and Chemistry* 2nd edn (Amsterdam: North-Holland)